

An Oxygen-Deficient Perovskite as Selective Catalyst in the Oxidation of Alkyl Benzenes**

A. Aguadero, H. Falcon, J. M. Campos-Martin, S. M. Al-Zahrani, J. L. G. Fierro, and J. A. Alonso*

The aerobic oxidation of hydrocarbons is a very important commercial process for the production of oxygen-containing compounds such as alcohols, aldehydes, ketones, carboxylic acids, and epoxides.^[1–4] However, the reaction conditions are often harsh, the reagent mixtures are corrosive (Cl^- or Br^-), and the reactions are frequently unselective. Therefore, the selective transformation of hydrocarbons, especially saturated hydrocarbons such as alkanes, to valuable oxygenated compounds constitutes an extremely important area of the contemporary industrial chemistry. Today, over 90% of organic chemicals are derived from petroleum, whose main components are saturated hydrocarbons.

An innovation in the aerobic oxidation of hydrocarbons through catalytic carbon radical generation under mild conditions has been achieved through the use of *N*-hydroxyphthalimide (NHPI) as a key compound, albeit requiring the presence of a transition-metal compound.^[5–11] In this oxidation, the phthalimide *N*-oxyl radical (PINO) generated in situ abstracts the hydrogen atom from the hydrocarbon to form an alkyl radical, which is readily trapped by dioxygen to form oxygenated compounds. The NHPI method is applicable in a broad variety of organic syntheses via carbon radical intermediates.^[5–11] A key challenge is to develop an inexpensive heterogeneous catalyst for liquid-phase oxidation of alkyl aromatics with an oxygen containing gas with high conversion rate and selectivity.

Oxygen-deficient $\text{ABO}_{3-\delta}$ perovskites have been reported to present high catalytic activity in oxidation reactions.^[12,13]

These phases have been usually described with oxygen stoichiometries equal to or higher than 2.5 in compositions ranging from ABO_3 to $\text{ABO}_{2.5}$. It is generally observed that these deviations of stoichiometry can be supported almost without changing the building blocks of the perovskite structure even though the anionic defects may form disordered or vacancy-ordered structures. Only a few members of the wide family of perovskite oxides have been obtained with values of $\delta > 0.5$, in which the three dimensional array of the perovskite structure is maintained; most of them are Co-based perovskites of the $\text{Sr}_{1-y}\text{Ba}_y\text{CoO}_{3-\delta}$ family.^[14–17]

In this work we have developed a new oxygen-defective $(\text{La,Sr})_{0.5}(\text{Mn,Co})_{0.5}\text{O}_{3-\delta}$ heterogeneous catalyst with high conversion and selectivity in the heterogeneous oxidation of alkyl aromatics. The obtained perovskite presents a wide range of oxygen stoichiometries and is ferromagnetic at room temperature.

The oxygen-stoichiometric $(\text{La,Sr})_{0.5}(\text{Mn,Co})_{0.5}\text{O}_3$ perovskite oxide was obtained as a well-crystallized black polycrystalline powder. Figure 1 displays the thermogravimetric curve corresponding to the reduction process to obtain the hypostoichiometric phase; a weight loss of $\delta = 0.62$ oxygen atoms per formula unit was observed. The XRD patterns of the stoichiometric and hypostoichiometric samples are included in Figure S1a,b in the Supporting Information.

The crystal structure of the oxidized sample was successfully Rietveld-refined in the rhombohedral $R\bar{3}c$ space group with oxygen content of 2.98(2) per formula unit (Figure 2a) from neutron powder diffraction (NPD) data, revealing that the material is not ordered in a cubic $Fm\bar{3}m$ space group as previously stated from X-ray diffraction results.^[18,19] As for

[*] Dr. A. Aguadero, Prof. Dr. J. A. Alonso
Instituto de Ciencia de Materiales de Madrid, CSIC
Cantoblanco, 28049 Madrid (Spain)
Fax: (+34) 91-372-0623
E-mail: ja.alonso@icmm.csic.es
Homepage: <http://www.icmm.csic.es/jaalonso>
Dr. H. Falcon, Dr. J. M. Campos-Martin, Prof. Dr. J. L. G. Fierro
Sustainable Energy and Chemistry Group (EQS)
Instituto de Catálisis y Petroquímica, CSIC
Marie Curie, 2 Cantoblanco, 28049 Madrid (Spain)
Prof. Dr. S. M. Al-Zahrani
Chemical Engineering Department, College of Engineering
King Saud University, Riyadh (Kingdom of Saudi Arabia)

[**] We thank our research sponsor The King Saud University, Riyadh (Saudi Arabia). We acknowledge the financial support of the Spanish Ministry of Innovation and Science for the projects (MAT2010-16404, CT02010-19157-C03-01). We are grateful to Institut Laue-Langevin for making facilities available. A.A. thanks MICINN for a "Juan de la Cierva" contract.

Supporting information for this article is available on the WWW under <http://dx.doi.org/10.1002/ange.201007941>.

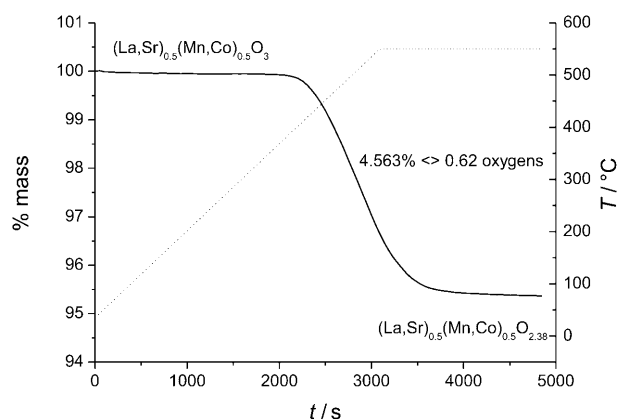


Figure 1. Thermogravimetric analysis under 5% H_2 /95% N_2 flow of the stoichiometric $(\text{La,Sr})_{0.5}(\text{Mn,Co})_{0.5}\text{O}_3$.

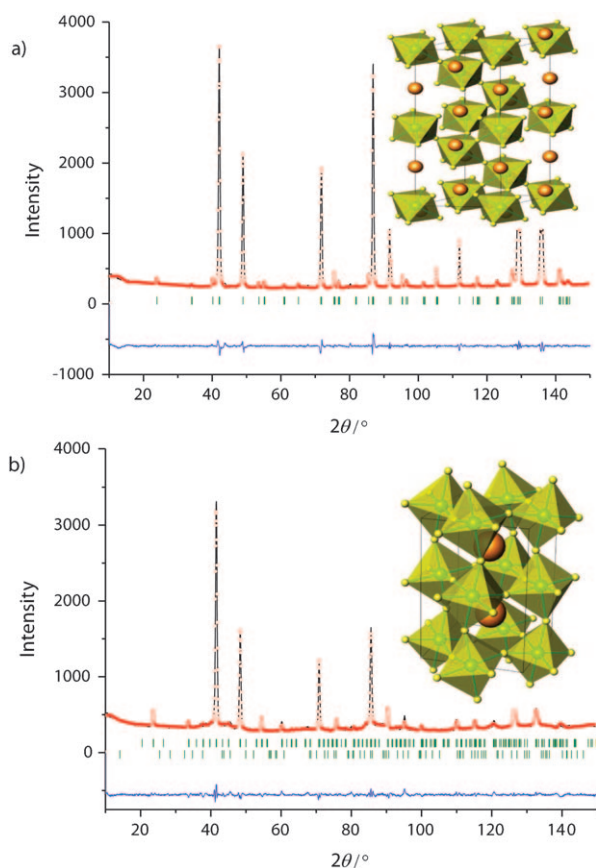


Figure 2. Observed (circles), calculated (full line), and difference (bottom) NPD Rietveld profiles for a) $(\text{La,Sr})_{0.5}(\text{Mn,Co})_{0.5}\text{O}_{2.98(2)}$ (air-prepared) at room temperature, after the refinement in the $R\bar{3}c$ space group; $(\text{Mn,Co})\text{--O}$ distance 1.9280(5) Å; b) $(\text{La,Sr})_{0.5}(\text{Mn,Co})_{0.5}\text{O}_{2.52(2)}$ (reduced) at 423 K, refined in the $Pbnm$ space group; average distance $(\text{Mn,Co})\text{--O}$ = 1.948(1) Å. Vertical lines correspond to the Bragg positions for pure compound (top) and LaSrMnO_4 secondary phase (bottom). The insets illustrate the rhombohedral $R\bar{3}c$ and orthorhombic $Pbnm$ crystal structures for the oxidized and reduced perovskite oxides.

the reduced compound, the NPD study reveals a slight deviation from the cubic symmetry that can be structurally defined in the $Pbnm$ space group, with a random distribution of the metals over the A and B positions of the perovskite and oxygen vacancies (Figure 2b). A minor LaSrMnO_4 impurity with K_2NiF_4 -type structure was observed. It is worth noting that the oxygen-hypostoichiometric perovskite is easily oxidized even at ambient conditions, where it superficially uptakes some oxygen; for this reason the NPD data collected at room temperature showed an admixture with the oxidized phase (Figure S2 in the Supporting Information). However, the NPD pattern collected at 423 K under vacuum conditions corresponded to a single reduced perovskite phase with slight amount of LaSrMnO_4 as secondary phase. The quantity of oxygen refined in the structure is $\text{O}_{2.52(2)}$ with high values of isotropic thermal factors ($2.7(2) \text{ \AA}^2$ for O1 and $5.3(1) \text{ \AA}^2$ for O2), which might indicate a huge mobility of oxide ion in this structure; standard values of thermal displacements of oxygen in perovskite oxides are around 1 \AA^2 at room temperature.

The re-oxygenation of the sample happens in at least two subsequent processes (Figure S3 in the Supporting Information) with concomitant oxidation of the transition-metal cations from an average oxidation state of +2.54 for the partially oxidized sample to +3.42 in the intermediate stage and +3.56 in the totally oxidized sample. These oxidation states were confirmed by XPS analysis (Figure S4 and Table S1 in the Supporting Information).

The reduction of the sample is mirrored by the shift of the binding energy of $\text{Mn}2p_{3/2}$ and $\text{Co}2p_{3/2}$ core levels from 642.0 to 641.2 eV and 781.1 to 779.2 eV, respectively. Figure 3 shows

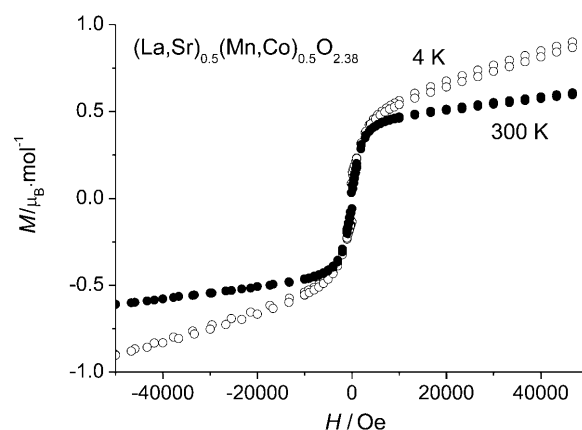


Figure 3. Magnetization versus field isotherms at $T = 4 \text{ K}$ and 300 K for the reduced phase.

the magnetization isotherms of the reduced sample at 4 and 300 K; both curves are characteristic of a ferromagnet with a Curie temperature above room temperature. The oxidized sample is ferromagnetic below 225 K as previously reported;^[18,19] it seems that the reduction of the sample promotes the increment of the magnetic interactions and the Curie temperature, despite the presence of a large number of oxygen vacancies that would perturb the double exchange through $(\text{Mn,Co})\text{--O}\text{--}(\text{Mn,Co})$ paths.

These materials have been used as catalysts in the oxidation of several alkyl aromatic compounds. Very interesting results were obtained in the oxidation of *p*-xylene. This reaction was carried out using various catalytic systems— $(\text{La,Sr})_{0.5}(\text{Mn,Co})_{0.5}\text{O}_{3-\delta}/\text{NHPI}$, $(\text{La,Sr})_{0.5}(\text{Mn,Co})_{0.5}\text{O}_3/\text{NHPI}$ —and, for comparative purposes to benchmark the present state of the art, we employed $\text{Co}(\text{OAc})_2/\text{Mn}(\text{OAc})_2/\text{NHPI}$, which is the best catalytic system described in literature for soft reaction conditions.^[6–8] The *p*-xylene conversion was 100% for all the systems (Table 1). However, the product distribution is highly affected by the catalyst used. In all cases, three main products were obtained: *p*-toluic acid (*p*-TOA), 4-carboxybenzaldehyde, and the desired product terephthalic acid (TPA). TPA is the industrial product of interest because it is one of the reactants used in the production of PET (polyethylene terephthalate). The most interesting results were obtained with the hypostoichiometric sample, which promotes a great yield to terephthalic acid (99%) produced with only 0.9% of *p*-toluic acid (Table 1).

Table 1: Products of the oxidation of *p*-xylene for 5 h.

| Catalyst | <i>p</i> -Xylene conversion [%] | Product distribution [%] | |
|---|---------------------------------|--------------------------|------|
| | | <i>p</i> -TOA | TPA |
| NHPI/Co(OAc) ₂ /Mn(OAc) ₂ | 100.0 | 19.0 | 81.0 |
| NHPI/(La,Sr) _{0.5} (Mn,Co) _{0.5} O ₃ | 100.0 | 33.0 | 67.0 |
| NHPI/(La,Sr) _{0.5} (Mn,Co) _{0.5} O _{3-δ} | 100.0 | 0.9 | 99.1 |

Figure 4 illustrates the temporal product distribution obtained by examining the concentration time course profiles of each product. The *p*-xylene consumption rate was high and similar for all catalysts, and no *p*-xylene was detected at reaction times over 1 h. The concentration of the intermediate

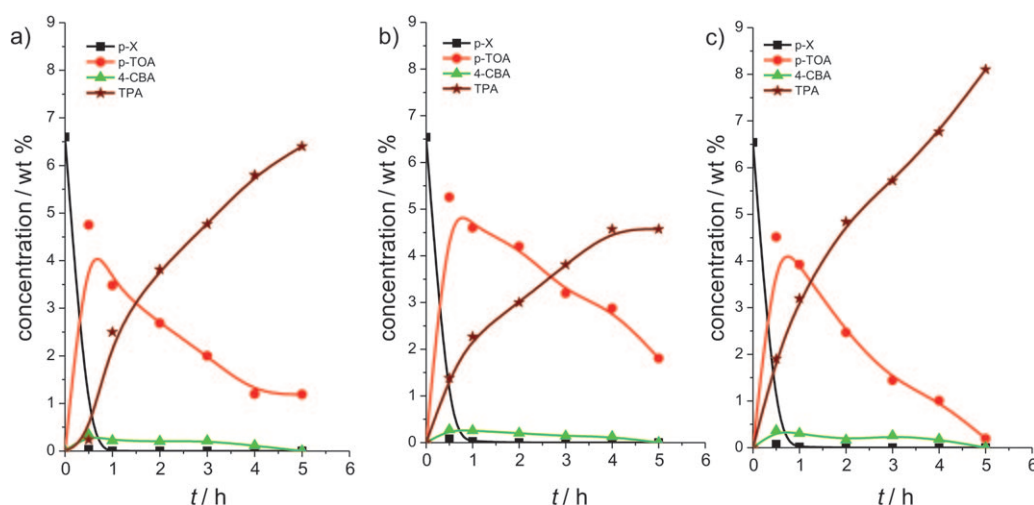


Figure 4. Concentration profiles of the main components identified in the oxidation of *p*-xylene at 20 bar O₂ and 363 K using: a) NHPI/Co(OAc)₂/Mn(OAc)₂, b) NHPI/(La,Sr)_{0.5}(Mn,Co)_{0.5}O₃, and c) NHPI/(La,Sr)_{0.5}(Mn,Co)_{0.5}O_{3-δ} catalytic systems.

p-TOA product increases quickly at short reaction times; in parallel, the *p*-xylene consumption reaches a maximum in a time interval of 0.5–1 h and then decreases for reaction times longer than 1 h. This behavior is typical of consecutive reactions in which one or more intermediate products are formed before they are transformed into the final one, namely TPA in this case. The peak concentration and the shape of *p*-TOA and TPA profiles depend on the catalyst used. The *p*-TOA concentration decreases quickly on the oxidized (La,Sr)_{0.5}(Mn,Co)_{0.5}O₃ catalyst but more slowly than observed with the homogenous Co(OAc)₂/Mn(OAc)₂ reference catalyst.

Interestingly, the hypostoichiometric (La,Sr)_{0.5}(Mn,Co)_{0.5}O_{3-δ} catalyst counterpart displays the highest *p*-TOA disappearance rate and subsequently the highest TPA formation rate. According to these profiles, the formation rate of TPA follows the trend: (La,Sr)_{0.5}(Mn,Co)_{0.5}O₃ < Co(OAc)₂/Mn(OAc)₂ < (La,Sr)_{0.5}(Mn,Co)_{0.5}O_{3-δ}. These results clearly indicate that the hypostoichiometric perovskite facilitates the global oxidation process; summing up, it is a more efficient oxidizing catalyst.

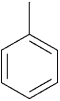
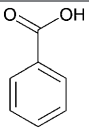
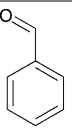
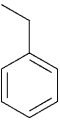
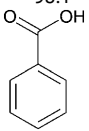
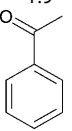
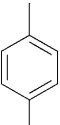
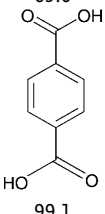
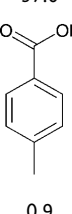
The large difference in reactivity towards TPA formation of both perovskite catalysts seems to be related to their ability to favor the oxidation of *p*-TOA and thus it should be related to their oxygen vacancy concentration and the oxidation states of Co and Mn. The hypostoichiometric perovskite ((La,Sr)_{0.5}(Mn,Co)_{0.5}O_{3-δ}) is able to accommodate a wide variety of oxygen stoichiometries and therefore different oxidation states for Co and Mn, favoring the charge transfer in the oxidation reaction. In contrast, the presence of a high number of oxygen vacancies could favor the activation of the NHPI to form the phthalimide *N*-oxyl radical (PINO), promoting the absorption of the hydrogen atom from the hydrocarbon to form an alkyl radical, which reacts with O₂ molecules to afford oxygenated compounds.^[6–11]

The hypostoichiometric perovskite was also very efficient in the aerobic oxidation of other alkyl aromatics (toluene or ethylbenzene; Table 2). In both cases, the conversion of alkyl aromatics was very high (>99.5%). The selectivity in the oxidation of toluene was 98% and 2% to benzoic acid and benzaldehyde, respectively. Surprisingly, the oxidation of ethylbenzene produced mainly benzoic acid (63%) and acetophenone (37%); this product distribution is different from that usually published, whereby the main product is acetophenone, a stable product against soft oxidation conditions.^[20,21] These results indicate again that the hypostoichiometric perovskite is more effective than standard catalytic systems for the oxidation of organic substrates, because with NHPI/(La,Sr)_{0.5}(Mn,Co)_{0.5}O_{3-δ} we were able to continue the oxidation of ethylbenzene beyond acetophenone to yield benzoic acid.

The hypostoichiometric perovskite was reused twice in the oxidation of ethylbenzene; the conversion rate was virtually unchanged, and the selectivity continued to be reasonably good (Figure S5). XRD analysis of the used sample (Figure S1c) showed a perovskite structure with unit-cell parameters corresponding to the reduced specimen.

In conclusion, we have prepared an extremely oxygen-defective perovskite oxide of composition (La,Sr)_{0.5}(Mn,Co)_{0.5}O_{2.38} by topotactic reduction of an oxygen-stoichiometric specimen (La,Sr)_{0.5}(Mn,Co)_{0.5}O₃. The crystal structures of both materials were studied by NPD analysis; the structure of the reduced oxide presents a subtle orthorhombic distortion, and the metals as well as the oxygen vacancies are distributed randomly over the corresponding sublattices. The

Table 2: Products of the oxidation of alkyl aromatics at 20 bar O₂ after 3 h of reaction over NHPI/(La,Sr)_{0.5}(Mn,Co)_{0.5}O_{3-δ} (#948).

| Substrate | Conv. [%] | Product distribution [%] | |
|---|-----------|--|--|
|  | 99.7 |  98.1 |  1.9 |
|  | 99.8 |  63.0 |  37.0 |
|  | 100 |  99.1 |  0.9 |

hypostoichiometric material shows an extraordinary reaction rate and selectivity for the conversion of alkyl aromatics, for example, *p*-xylene in TPA, with respect to the standard homogeneous catalyst. The fact that this (La,Sr)_{0.5}(Mn,Co)_{0.5}O_{2.38} perovskite phase is ferromagnetic above room temperature constitutes an added advantage, since it could be separated from the solid product with a magnet; the mother liquor could be removed by filtration to yield pure TPA.

Experimental Section

The oxygen-stoichiometric (La,Sr)_{0.5}(Mn,Co)_{0.5}O₃ oxide was obtained by a nitrate–citrate route followed by a heat treatment at 1150 °C 12 h in air. The subsequent reduction of the polycrystalline powder at 520 °C for 8 h in H₂/N₂ (5%/95%) forming gas promotes the formation of the extremely oxygen-defective (La,Sr)_{0.5}(Mn,Co)_{0.5}O_{2.38} perovskite. Thermal analysis was carried out in a Mettler TA3000 system equipped with a TC10 processor unit. Thermogravimetric (TG) curves were obtained in a TG50 unit, working at a heating rate of 10 °C min⁻¹ in an H₂/N₂ (5%/95%) or O₂ flow of 0.3 L min⁻¹. The initial characterization of the products was carried out by laboratory X-ray diffraction (XRD) with a Bruker-axs D8 Advanced diffractometer (40 kV, 30 mA) with Cu K_α radiation ($\lambda = 1.5418$ Å) and a PSD (position sensitive detector). The crystallographic structures of the oxidized and reduced samples were refined from high-resolution neutron powder diffraction (NPD) patterns collected at the Institut Laue-Langevin (ILL) in Grenoble (France), acquired at 295 and 423 K at the D2B diffractometer with $\lambda = 1.594$ Å. The high-intensity mode was used; the collection time was 2 h. The refinement of the crystal structure was performed by the Rietveld method, using the FULLPROF refinement program^[22] and its internal tables for the coherent scattering lengths of the corresponding elements. The peak profiles were fitted by the Thompson–Cox–Hastings pseudo-Voigt function corrected for axial divergence asymmetry. The following parameters were refined in the final run: scale factor, background coefficients, zero-point error, pseudo-Voigt corrected for asymmetry parameters, positional coordinates, and anisotropic thermal factors.

Magnetic measurements were carried out in a Quantum-Design SQUID magnetometer; magnetization isotherms were collected at 4 and 300 K between –50 kOe and +50 kOe. Photoelectron spectra were recorded with a VG Escalab 200R electron spectrometer provided with MgK_α X-ray source and a hemispherical electron analyzer. The binding energies were referenced to the C1s peak at 284.9 eV. Data processing was performed with the XPS peak program, and the spectra were decomposed with the least-squares fitting routine provided with the software with Gaussian/Lorentzian (90/10) lines and after subtracting a Shirley background.

The oxidation of alkyl aromatics was performed in a 100 mL steel autoclave (autoclave Engineers). In a typical run, 1.46 g of substrate, 0.435 g of *N*-hydroxyphthalimide, 50 mg of perovskite or 0.0166 g of cobalt(II) acetate, 0.0115 g of manganese(II) acetate, and 20 mL of acetic acid were mixed together. The reactor was pressurized with oxygen at 20 bar and the temperature was set to 363 K. Then, the stirring was started and set at 1000 rpm. The pressure was maintained at 20 bar, and fresh oxygen was fed in as it was consumed. The liquid was analyzed by gas chromatography with a flame ionization detector (GC-FID) on an Agilent 6850 device equipped with an HP-WAX column. Crystallographic data for oxidized (La,Sr)_{0.5}(Mn,Co)_{0.5}O₃: *R*3̄c, hexagonal setting, $a = 5.4463(5)$ Å, $c = 13.2885(2)$ Å, $V = 341.355(6)$ Å³, O1 ($x, 0, \frac{1}{4}$) $x = 0.4745(1)$, $\rho_{\text{calcd}} = 8.386$ g cm⁻³, $Z = 6$, $R_{\text{wp}} = 3.19\%$, $R_{\text{p}} = 2.42\%$, $R_{\text{exptl}} = 1.95\%$, $\chi^2 = 2.68$, $R_{\text{Bragg}} = 2.55\%$, measurement range $10^\circ \leq 2\theta \leq 160^\circ$, 3198 data points, 80 observed reflections, 68 parameters refined. Crystallographic data for reduced (La,Sr)_{0.5}(Mn,Co)_{0.5}O_{2.38} at 423 K: *Pbnm*, $a = 5.5071(4)$ Å, $b = 5.4873(5)$ Å, $c = 7.7898(6)$ Å, $V = 235.40(3)$ Å³, $\rho_{\text{calcd}} = 7.890$ g cm⁻³, $Z = 4$, $R_{\text{wp}} = 3.22\%$, $R_{\text{p}} = 2.48\%$, $R_{\text{exptl}} = 1.85\%$, $\chi^2 = 3.05$, $R_{\text{Bragg}} = 8.38\%$, measurement range $10^\circ \leq 2\theta \leq 160^\circ$, 3198 data points, 254 observed reflections, 23 parameters refined. Further details on the crystal structure investigation may be obtained from the Fachinformationszentrum Karlsruhe, 76344 Eggenstein-Leopoldshafen, Germany (fax: (+49) 7247-808-666; e-mail: crysdata@fiz-karlsruhe.de), on quoting the depository numbers CSD-422410 and -422411 for the oxidized and reduced phases, respectively.

Received: December 15, 2010

Revised: April 13, 2011

Published online: May 31, 2011

Keywords: heterogeneous catalysis · magnetic properties · neutron diffraction · oxidation · perovskite phases

- [1] I. Hermans, J. Peeters, P. A. Jacobs, *Top. Catal.* **2008**, *50*, 124.
- [2] P. P. Toribio, J. M. Campos-Martin, J. L. G. Fierro, *J. Mol. Catal. A* **2005**, *227*, 101.
- [3] P. P. Toribio, J. M. Campos-Martin, J. L. G. Fierro, *Appl. Catal. A* **2005**, *294*, 290.
- [4] L. Barrio, P. P. Toribio, J. M. Campos-Martin, J. L. G. Fierro, *Tetrahedron* **2004**, *60*, 11527.
- [5] P. P. Toribio, A. Gimeno-Gargallo, M. C. Capel-Sanchez, M. P. de Frutos, J. M. Campos-Martin, J. L. G. Fierro, *Appl. Catal. A* **2009**, *363*, 32.
- [6] Y. Ishii, S. Sakaguchi, T. Iwahama, *Adv. Synth. Catal.* **2001**, *343*, 393.
- [7] R. A. Sheldon, I. W. C. E. Arends, *Adv. Synth. Catal.* **2004**, *346*, 1051.
- [8] Y. Ishii, S. Sakaguchi, *Catal. Today* **2006**, *117*, 105.
- [9] H. Falcon, J. M. Campos-Martin, S. M. Al-Zahrani, J. L. G. Fierro, *Catal. Commun.* **2010**, *12*, 5.
- [10] R. A. Sheldon, I. W. C. E. Arends, *J. Mol. Catal. A* **2006**, *251*, 200.
- [11] F. Recupero, C. Punta, *Chem. Rev.* **2007**, *107*, 3800.
- [12] L. G. Tejuca, J. L. G. Fierro, J. M. D. Tascon, *Adv. Catal.* **1989**, *36*, 237.

- [13] M. A. Peña, J. L. G. Fierro, *Chem. Rev.* **2001**, *101*, 1981.
 - [14] Y. Takeda, R. Kanno, T. Takada, O. Yamamoto, *Z. Anorg. Allg. Chem.* **1986**, *540*, 259.
 - [15] V. V. Vashook, M. V. Zinkevich, Y. G. Zonov, *Solid State Ionics* **1999**, *116*, 129.
 - [16] C. De La Calle, J. A. Alonso, A. Aguadero, M. T. Fernandez-Diaz, F. Porcher, *Z. Kristallogr.* **2010**, *225*, 209.
 - [17] C. de La Calle, J. A. Alonso, A. Aguadero, M. T. Fernandez-Diaz, *Dalton Trans.* **2009**, 4104.
 - [18] A. Androulakis, N. Katsarakis, J. Giapintzakis, N. Vouroutzis, E. Pavlidou, K. Chrissafis, E. K. Polychroniadis, V. Perdikatis, *J. Solid State Chem.* **2003**, *173*, 350.
 - [19] R. N. Mahato, K. Sethupathu, V. Sankaranarayanan, K. K. Bharathi, R. Nirmala, A. K. Nigam, S. K. Malik, *IEEE Trans. Magn.* **2009**, *45*, 4271.
 - [20] K. R. Seddon, A. Stark, *Green Chem.* **2002**, *4*, 119.
 - [21] T. Mallat, A. Baiker, *Chem. Rev.* **2004**, *104*, 3037.
 - [22] J. Rodríguez-Carvajal, *Physica B* **1993**, *192*, 55.
-